

# A SPIN NETWORK PRIMER

SETH A. MAJOR

ABSTRACT. Spin networks, essentially labeled graphs, are “good quantum numbers” for the quantum theory of geometry. These structures encompass a diverse range of techniques which may be used in the quantum mechanics of finite dimensional systems, gauge theory, and knot theory. Though accessible to undergraduates, spin network techniques are buried in more complicated formulations. In this paper a diagrammatic method, simple but rich, is introduced through an association of  $2 \times 2$  matrices to diagrams. This spin network diagrammatic method offers new perspectives on the quantum mechanics of angular momentum, group theory, knot theory, and even quantum geometry. Examples in each of these areas are discussed.

## 1. INTRODUCTION

Originally introduced as a quantum model of spatial geometry [1], spin networks have recently been shown to provide both a natural home for geometric operators [2] and a basis for the states of quantum gravity kinematics [3]. At their roots, spin networks provide a description of the quantum mechanics of two-state systems. Even with this humble foundation, spin networks form a remarkably diverse structure which is useful in knot theory, the quantum mechanics of angular momentum, quantum geometry, and other areas.

Spin networks are intrinsically accessible to undergraduates, but much of the the material is buried in more complex formulations or lies in hard-to-find manuscripts. This article is intended to fill this gap. It presents an introduction to the diagrammatic methods of spin networks, with an emphasis on applications in quantum mechanics. In so doing, it offers undergraduates not only a fresh perspective on angular momentum in quantum mechanics but also a link to leading edge research in the study of the Hamiltonian formulation of quantum gravity. One quantum operator of geometry is presented in detail; this is the operator which measures the area of a surface.

The history of spin networks goes back to the early seventies when Penrose first constructed networks as a fundamentally discrete model for three-dimensional space [1]. Difficulties inherent in the continuum formulation of physics led Penrose to explore this possibility.<sup>1</sup> These difficulties come from both quantum and gravitational theory as seen from three examples: First, while quantum physics is based on noncommuting quantities, coordinates of space are commuting numbers, so it appears that our usual notion of space conflicts with quantum mechanics. Second, on a more pragmatic level, quantum calculations often yield divergent answers which grow arbitrarily large as one calculates physical quantities on finer and smaller scales. A good bit of machinery in quantum field theory is devoted to regulating and renormalizing these divergent quantities. However, many of these difficulties vanish if a smallest size or “cut-off” is introduced. A discrete structure, such as a lattice, provides such a cut-off. Thus, were spacetime built from a lattice or network, then quantum field theory would be spared much of the problems of divergences. Third, there is a hint coming from general relativity itself. Since regular initial data, say a collapsing shell of matter, can evolve into a singularity, relativity demonstrates

---

*Date:* August 1999; Revised 2010.

<sup>1</sup>There are more philosophic motivations for this model as well. Mach advocated an interdependence of phenomena: “The physical space I have in mind (which already includes time) is therefore nothing but the dependence of the phenomena on one another. A completed physics that knew of this dependence would have no need of separate concepts of space and time because these would already have be encompassed” [4] echoing Leibniz’s much earlier critique of Newton’s concept of absolute space and time. Penrose invokes such a Machian principle: A background space on which physical events unfold should not play a role; only the relationships of objects to each other can have significance [1].

that the spacetime metric is not always well-defined. This suggests that it is profitable to study other methods to model spacetime. As the absolute space and time of Newton is a useful construct to apply in many everyday calculations, perhaps continuous spacetime is simply useful as a calculational setting for a certain regime of physics.

Motivated by these difficulties, Penrose constructed a discrete model of space. The goal was to build a consistent model from which classical, continuum geometry emerged only in a limit. Together with John Moussouris he was able to show that spin networks could reproduce the familiar 3 dimensional angles of space – a “theory of quantized directions” [5]. In this setting, spin networks were trivalent graphs labeled by spins.

Later, spin networks were re-discovered by Rovelli and Smolin when they were searching for the eigenspace of operators measuring geometric quantities such as area and volume [2], [6]. In this setting spin networks had to be generalized to include graphs with higher valence vertices. This early work launched many studies which resulted in a powerful suite of spin network techniques for background-independent quantization.

Spin networks are fantastically useful both as a basis for the states of quantum geometry and as a computational tool. Spin network techniques were used to compute the spectrum of area [6] and volume [7] operators. Spin networks, first used as a combinatorial basis for spacetime, find application in quantum gravity, knot theory, and group theory.

This spin network primer begins by associating  $2 \times 2$  matrices with diagrams. The first goal is to make the diagrammatics “planar isotopic,” meaning the diagrams are invariant under smooth deformations of lines in the plane. It is analogous to the manipulations which one would expect for ordinary strings on a table. Once this is completed, the structure is enriched in Section 2.3 to allow combinations and intersections between lines. This yields a structure which includes the rules of addition of angular momentum. It is further explored in Section 3 with the diagrammatics of the usual angular momentum relations of quantum mechanics. (A reader more familiar with the angular momentum states of quantum mechanics may wish to go directly to this section to see how spin networks are employed in this setting.) In Section 4 this connection to angular momentum is used to give a diagrammatic version of the Wigner-Eckart theorem. The article finishes with a discussion on the area operator of quantum gravity.

## 2. A PLAY ON LINE

This section begins by building an association between the Kronecker delta functions the  $2 \times 2$  identity matrix (or  $\delta_A^B$ ) and a line. It is not hard to ensure that the lines behave like elastic strings on a table. The association and this requirement leads to a little bit of knot theory, to the full structure of spin networks, and to a diagrammatic method for the quantum mechanics of angular momentum.

**2.1. Line, bend and loop.** The Kronecker  $\delta_A^B$  is the  $2 \times 2$  identity matrix in component notation. Thus,

$$(\delta_A^B) = \begin{pmatrix} 1 & 0 \\ 0 & 1 \end{pmatrix}$$

and  $\delta_0^0 = \delta_1^1 = 1$  while  $\delta_0^1 = \delta_1^0 = 0$ . The Latin capital indices,  $A$  and  $B$  in this expression, may take one of two values 0 or 1. The diagrammatics begins by associating the Kronecker  $\delta$  to a line

$$\delta_A^B \sim \left. \vphantom{\delta_A^B} \right|_A^B.$$

The position of the indices on  $\delta$  determines the location of the labels on the ends of the line. Applying the definitions one has

$$\left. \vphantom{\delta_A^B} \right|_1^1 = 1 \text{ and } \left. \vphantom{\delta_A^B} \right|_0^0 = 0.$$

If a line is the identity then it is reasonable to associate a curve to a matrix with two upper (or lower) indices. There is some freedom in the choice of this object. As a promising possibility, one can

choose the antisymmetric matrix  $\epsilon_{AB}$

$$(\epsilon_{AB}) = (\epsilon^{AB}) = \begin{pmatrix} 0 & 1 \\ -1 & 0 \end{pmatrix}$$

so that

$$\epsilon_{AB} \sim \begin{array}{c} \text{---} \text{---} \\ \text{A} \quad \text{B} \end{array} .$$

Similarly,

$$\epsilon^{AB} \sim \begin{array}{c} \text{A} \quad \text{B} \\ \text{---} \text{---} \end{array} .$$

As a bent line is a straight line “with one index lowered” this choice fits well with the diagrammatics:  $\delta_A^C \epsilon_{CB} = \epsilon_{AB}$ .

After a bit of experimentation with these identifications, one discovers two awkward features. The diagrams do not match the expected moves of elastic strings in a plane. First, since  $\delta_A^C \epsilon_{CD} \epsilon^{DE} \delta_E^B = \epsilon_{AD} \epsilon^{DB} = -\delta_A^B$ , straightening a line yields a negative sign:

$$\begin{array}{c} \text{B} \\ \text{---} \\ \text{A} \end{array} = - \begin{array}{c} \text{B} \\ \text{---} \\ \text{A} \end{array} . \tag{1}$$

Second, as a consequence of  $\epsilon_{AD} \epsilon_{BC} \epsilon^{CD} = -\epsilon_{AB}$ ,

$$\begin{array}{c} \text{---} \text{---} \\ \text{A} \quad \text{B} \end{array} = - \begin{array}{c} \text{---} \text{---} \\ \text{A} \quad \text{B} \end{array} . \tag{2}$$

However, these “topological” difficulties are fixed by modifying the definition of a bent line. One can add an  $i$  to the antisymmetric tensors

$$\epsilon_{AB} \rightarrow \tilde{\epsilon}_{AB} = i\epsilon_{AB} \text{ so that } \tilde{\epsilon}_{AB} = \begin{array}{c} \text{---} \text{---} \\ \text{A} \quad \text{B} \end{array} .$$

Since each of the two awkward features contains a pair of  $\epsilon$ 's the  $i$  fixes these sign problems. However, there is one more property to investigate.

On account of the relation  $\delta_A^D \delta_B^C \tilde{\epsilon}_{CD} = -\tilde{\epsilon}_{AB}$  one has (The indices  $C$  and  $D$  are added to the diagram for clarity.)

$$\begin{array}{c} \text{C} \quad \text{D} \\ \text{---} \text{---} \\ \text{A} \quad \text{B} \end{array} = - \begin{array}{c} \text{---} \text{---} \\ \text{A} \quad \text{B} \end{array}$$

– not what one would expect for strings. This final problem can be cured by associating a minus sign to each crossing.

Thus, by associating an  $i$  to every  $\epsilon$  and a sign to every crossing, the diagrams behave as continuously deformed lines in a plane [1]. The more precise name of this concept is known as planar isotopy. Structures which can be moved about in this way are called topological. What this association of curves to  $\delta$ 's and  $\tilde{\epsilon}$ 's accomplishes is that it allows one to perform algebraic calculations by moving lines in a plane.

A number of properties follow from the above definitions. The value of a simple closed loop takes a negative value<sup>2</sup>

$$\bigcirc = -2, \tag{3}$$

since  $\tilde{\epsilon}_{AB} \tilde{\epsilon}^{AB} = -\epsilon_{AB} \epsilon^{AB} = -2$ ; a closed line is a number. This turns out to be a generic result in that a spin network which has no open lines is equivalent to a number.

A surprisingly rich structure emerges when crossings, are considered. For instance the identity, often called the “spinor identity,” links a pair of epsilons to products of deltas

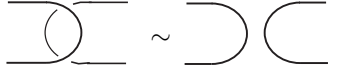
$$\epsilon_{AC} \epsilon^{BD} = \delta_A^B \delta_C^D - \delta_A^D \delta_C^B.$$

---

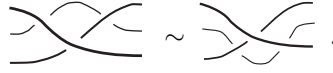
<sup>2</sup>This led Penrose to dub these “negative dimensional tensors” [1]. In general relativity, the dimension of a space is given by the trace of the metric,  $g_{\mu\nu} g^{\mu\nu}$ , hence the name.



- **Move II:** The overlaps of distinct curves are not knotted



- **Move III:** One can perform planar deformations under (or over) a diagram



With a finite sequence of these moves the projection of a knot may be transformed into the projection of any other knot which is topologically equivalent to the original. If two knots may be expressed as the other with a sequence of these moves then the knots are called “isotopic.” Planar isotopy is generated by all four moves with the significant caveat that there are no crossings  $\times$ , only intersections  $\bowtie$ . Planar isotopy may be summarized as the manipulations one would expect for elastic, non-sticky strings on a table top – if they are infinitely thin.

Move I on real strings introduces a twist in the string. This move is violated by any line which has some spatial extent in the transverse direction such as ribbons. Happily, there are diagrammatic spin networks for these “ribbons” as well [11], [12].

**2.3. Weaving and joining.** The skein relations of Eq. (4) show that, given a pair of lines there is one linear relation among the three quantities:  $\left| \begin{array}{c} | \\ | \end{array} \right|$ ,  $\left| \begin{array}{c} \diagup \\ \diagdown \end{array} \right|$ , and  $\left| \begin{array}{c} \diagdown \\ \diagup \end{array} \right|$ . So a set of graphs may satisfy many linear relations. It would be nice to select a basis which is independent of this identity. After some work, this may be accomplished by choosing the antisymmetric combinations of the lines – “weaving with a sign.”<sup>5</sup> The simplest example is for two lines

$$\left| \begin{array}{c} | \\ | \end{array} \right| = \frac{1}{2} \left( \left| \begin{array}{c} | \\ | \end{array} \right| - \left| \begin{array}{c} \diagdown \\ \diagup \end{array} \right| \right). \tag{5}$$

For more than two lines the idea is the same. One sums over permutations of the lines, adding a sign for each crossing. The general definition is

$$\left| \begin{array}{c} | \\ | \\ \vdots \\ | \end{array} \right| := \frac{1}{n!} \sum_{\sigma \in S_n} (-1)^{|\sigma|} \left| \begin{array}{c} | \dots n \dots \\ \sigma_k \\ | \end{array} \right| \tag{6}$$

in which a  $\sigma$  represents one permutation of the  $n$  lines and  $|\sigma|$  is the minimum number of crossings for this permutation. The boxed  $\sigma$  in the diagram represents the action of the permutation on the lines. It can be drawn by writing  $1\ 2\ \dots\ n$ , then permutation just above it, and connecting the same elements by lines.

In this definition, the label  $n$  superimposed on the edge record the number of “strands” in the edge. Edge are usually labeled this way, though I will leave simple 1-lines unlabeled. Two other notations are used for this weaving with a sign

$$\left| \begin{array}{c} | \\ | \\ \vdots \\ | \end{array} \right| = \frac{1}{n!} \left| \begin{array}{c} | \dots n \dots \\ \sigma_k \\ | \end{array} \right|.$$

These antisymmetrizers have a couple of lovely properties, retacing and projection: The antisymmetrizers are “irreducible,” or vanish when a pair of lines is retraced

$$\left| \begin{array}{c} | \dots \cap \dots \\ | \end{array} \right| = 0. \tag{7}$$

which follows from the antisymmetry. Using this and the binor identity of Eq. (4) one may show that the antisymmetrizers are “projectors” (the combination of two is equal to one)

$$\frac{1}{n!} \left| \begin{array}{c} | \dots n \dots \\ \sigma_k \\ | \end{array} \right| = \left| \begin{array}{c} | \\ | \end{array} \right|.$$

---

<sup>5</sup>Note that, because of the additional sign associated to crossings, the “antisymmetrizer” symmetrizes the indices in the  $\delta\epsilon$  world.

Making the simplest closed diagram out of these lines gives the loop value often denoted as  $\Delta_n$

$$\bigcirc^n = \Delta_n = (-1)^n (n+1).$$

The factor  $n+1$  expresses the “multiplicity” of the number of possible “ $A$ -values” on an edge with  $n$  strands. Each line in the edge carries an index, which takes two possible values. To see this note that for an edge with  $a$  strands the sum of the indices  $A, B, C, \dots$  is  $0, 1, 2, \dots, a$ . So that the sum takes  $a+1$  possible values. One may show using the recursion relations for  $\Delta_n$ <sup>6</sup> that the loop value is equal to this multiplicity. As we will see in Section 3 the number of possible combinations is the dimension of the representation.

As an example of the loop value, the 2-loop, has value 3. This is easily checked using the relations for the basic loop value (Eq. (3)) and the expansion of the 2-line using the skein relation

$$\left| \begin{array}{c} | \\ 2 \\ | \end{array} \right\rangle = \left| \left( + \frac{1}{2} \right) \begin{array}{c} \cup \\ \cup \end{array} \right\rangle. \quad (8)$$

Edges may be further joined into networks by making use of internal trivalent vertices

The dashed circle is a magnification of the dot in the diagram on the left. Such dashed curves indicate spin network structure at a point. The “internal” labels  $i, j, k$  are positive integers determined by the external labels  $a, b, c$  via

$$i = (a + c - b)/2, \quad j = (a + b - c)/2, \quad \text{and} \quad k = (b + c - a)/2.$$

As in quantum mechanics the external labels must satisfy the triangle inequalities

$$a + b \geq c, \quad b + c \geq a, \quad a + c \geq b$$

and the sum  $a + b + c$  is an even integer. The necessity of these relations can be seen by drawing the strands through the vertex.

With this vertex one can construct many more complex networks. After the loop, the next simplest closed graph has two vertices,

$$\theta(a, b, c) = \bigcirc_{a,b,c}^a.$$

The general evaluation, given in the appendix, of this diagram is significantly more complicated. As an example I give the evaluation of  $\theta(1, 2, 1)$  using Eq. (8),

$$\begin{aligned} \bigcirc_{1,2,1}^1 &= \bigcirc_{1,2,1}^1 + \frac{1}{2} \bigcirc_{1,2,1}^1 \\ &= (-2)^2 + \frac{1}{2}(-2) = 3. \end{aligned}$$

One can build ever more complicated networks. In fact, one can soon land a dizzying array of networks. I have collected a small zoo in the appendix with full definitions.

Now all the elements are in place for the definition of spin networks. A spin network consist of a graph, with edges and vertices, and labels. The labels, associated edges, represent the number of strands woven into edges. Any vertex with more than three incident edges must also be labeled to specify a decomposition into trivalent vertices. The graphs of spin networks need not be confined to a plane. In a projection of a spin network embedded in space, the crossings which appear in the projection may be shown as in the Reidemeister moves with over-crossing “ $\times$ ” and under-crossing “ $\times$ ”.

<sup>6</sup>The loop value satisfies  $\Delta_0 = 1, \Delta_1 = -2$ , and  $\Delta_{n+2} = (-2)\Delta_{n+1} - \Delta_n$ .

### 3. ANGULAR MOMENTUM REPRESENTATION

As spin networks are woven from strands which take two values, it is well-suited to represent two-state systems. It is perhaps not surprising that the diagrammatics of spin networks include the familiar  $|jm\rangle$  representation of angular momentum. The notations are related as

$$\begin{aligned} |\frac{1}{2} \frac{1}{2}\rangle &= u^A \sim \begin{array}{c} \uparrow \\ | \\ \downarrow \end{array} \quad \text{and} \\ |\frac{1}{2} -\frac{1}{2}\rangle &= d^A \sim \begin{array}{c} \uparrow \\ | \\ \circ \end{array} . \end{aligned}$$

(Secretly, the “ $u$ ” for “up” tell us that the index  $A$  only takes the value 1. Likewise “ $d$ ” tells us the index is 0.) The inner product is given by linking upper and lower indices, for instance

$$\langle \frac{1}{2} \frac{1}{2} | \frac{1}{2} \frac{1}{2} \rangle \sim \begin{array}{c} | \\ \downarrow \\ \uparrow \\ | \end{array} = 1.$$

We can use these simple graphical structures to build up the representations  $|jm\rangle$  [5]

$$|j m\rangle := |r s\rangle = N_{rs} \underbrace{u^{(A} u^B \dots u^C}_r \underbrace{d^D d^E \dots d^F)}_s \quad (9)$$

in which

$$N_{rs} = \left( \frac{1}{r! s! (r+s)!} \right)^{1/2}, \quad j = \frac{r+s}{2}, \quad \text{and} \quad m = \frac{r-s}{2}. \quad (10)$$

The parentheses in Eq. (9) around the indices indicate symmetrization, e.g.  $u^{(A} d^B) = u^A d^B + u^B d^A$ . The normalization  $N_{rs}$  ensures that the states are orthonormal in the usual inner product.

This way of representing the states is also known as the Schwinger representation of the  $su(2)$  algebra in terms of two harmonic oscillators. In this case  $r$  is the level of one oscillator and  $s$  is the level of the second oscillator. [See gr-qc/0501075 and 0911.3553. Look up standard reference on Schwinger rep.]

A useful graphical representation of this state is in terms of the trivalent vertex. Using the notation “ $\wedge$ ” for  $u$  and similarly for  $d$  I have

$$|j m\rangle \sim \begin{array}{c} r+s \\ | \\ \wedge \\ \begin{array}{cc} \circ & \circ \end{array} \end{array} .$$

Angular momentum operators also take a diagrammatic form. As all spin networks are built from spin- $\frac{1}{2}$  states, it is worth exploring this territory first. Spin- $\frac{1}{2}$  operators have a representation in terms of the Pauli matrices

$$\sigma_1 = \begin{pmatrix} 0 & 1 \\ 1 & 0 \end{pmatrix}, \quad \sigma_2 = \begin{pmatrix} 0 & -i \\ i & 0 \end{pmatrix}, \quad \sigma_3 = \begin{pmatrix} 1 & 0 \\ 0 & -1 \end{pmatrix}$$

with

$$\hat{S}_i = \frac{\hbar}{2} \sigma_i$$

for  $i = 1, 2, 3$ . One has

$$\frac{\sigma_3}{2} |\frac{1}{2} \frac{1}{2}\rangle = \frac{1}{2} |\frac{1}{2} \frac{1}{2}\rangle,$$

which is expressed diagrammatically as

$$\begin{array}{c} \sigma_3 \\ | \\ \circ \end{array} = \frac{1}{2} \begin{array}{c} | \\ \circ \end{array} .$$

Or, since Pauli matrices are traceless,

$$\begin{array}{c} \sigma \\ \circ \end{array} = 0,$$

and using Eq (8) one has [14]

$$\begin{array}{c} \boxed{\sigma_3} \\ \circlearrowleft \\ \text{---}2\text{---} \\ | \\ \otimes \end{array} = \frac{1}{2} \begin{array}{c} | \\ \otimes \end{array}.$$

A similar relation holds for the states  $|\frac{1}{2} - \frac{1}{2}\rangle$ . The basic action of the spin operators can be described as a ‘‘hand’’ which acts on the state by ‘‘grasping’’ a line [13]. The result, after using the diagrammatic algebra, is either a multiple of the same state, as for  $\sigma_3$ , or a new state. If the operator acts on more than one line, a higher dimensional representation, then the total action is the sum of the graspings on each edge.<sup>7</sup>

The  $\hat{J}_z$  operator can be constructed out of the  $\sigma_3$  matrix. The total angular momentum  $z$ -component is the sum of individual measurements on each of the sub-systems.<sup>8</sup> In diagrams, the action of the  $\hat{J}_z$  operator becomes

$$\begin{aligned} \hat{J}_z |j m\rangle &\sim \begin{array}{c} \boxed{\sigma_3} \\ \circlearrowleft \\ \text{---}2\text{---} \\ | \\ \otimes \end{array} \rightarrow \begin{array}{c} r+s \\ | \\ \text{---}r\text{---}s\text{---} \\ \otimes \quad \otimes \end{array} \\ &= r \begin{array}{c} \boxed{\sigma_3} \\ \circlearrowleft \\ \text{---}2\text{---} \\ | \\ \otimes \end{array} \begin{array}{c} r+s \\ | \\ \text{---}r\text{---}s\text{---} \\ \otimes \quad \otimes \end{array} + s \begin{array}{c} \boxed{\sigma_3} \\ \circlearrowleft \\ \text{---}2\text{---} \\ | \\ \otimes \end{array} \begin{array}{c} r+s \\ | \\ \text{---}r\text{---}s\text{---} \\ \otimes \quad \otimes \end{array} \\ &= \hbar \left( \frac{r}{2} - \frac{s}{2} \right) \begin{array}{c} r+s \\ | \\ \text{---}r\text{---}s\text{---} \\ \otimes \quad \otimes \end{array} \\ &\equiv \hbar m |j m\rangle. \end{aligned}$$

The definition of the quantities  $r$  and  $s$  was used in the last line.

This same procedure works for the other angular momentum operators as well. The  $\hat{J}_x$  operator is constructed from the Pauli matrix  $\sigma_1$ . When acting on one line the operator  $\hat{J}_x$  matrix ‘‘flips the spin’’ and leaves a factor

$$\begin{array}{c} \boxed{J_x} \\ \circlearrowleft \\ \text{---} \\ | \\ \otimes \end{array} = \hbar \frac{1}{2} \begin{array}{c} | \\ \otimes \end{array}.$$

The reader is encouraged to try the same procedure for  $\hat{J}_y$ .

The raising and lowering operators are constructed with these diagrams as in the usual algebra. For the raising operator  $\hat{J}_+ = \hat{J}_1 + i\hat{J}_2$  one has

$$\hat{J}_+ |j m\rangle \sim \hbar s \begin{array}{c} r+s \\ | \\ \text{---}r+i\text{---}s-j\text{---} \\ \otimes \quad \otimes \end{array}.$$

In a similar way one can compute

$$\hat{J}_- \hat{J}_+ |j m\rangle = \hbar^2 (r+1)s |j m\rangle$$

from which one can compute the normalization of these operators: Taking the inner product with  $\langle j m |$  gives the usual normalization for the raising operator

$$\hat{J}_+ |j m\rangle = \hbar \sqrt{s(r+1)} |j m\rangle = \hbar \sqrt{(j-m)(j+m+1)} |j m\rangle.$$

<sup>7</sup>This may be shown by noticing that

$$\begin{array}{c} \text{---} \\ | \\ \otimes \end{array} = \begin{array}{c} \text{---} \\ | \\ \otimes \end{array}, \text{ so that } \begin{array}{c} \hbar \\ \text{---} \\ | \\ \otimes \end{array} + \begin{array}{c} \hbar \\ \text{---} \\ | \\ \otimes \end{array} + \dots = n \begin{array}{c} \hbar \\ \text{---} \\ | \\ \otimes \end{array},$$

as may be derived using Eqs. (4) and (7).

<sup>8</sup>The operator is  $\hat{J}_z = \hbar \sum_{i=1}^{2j+1} 1 \otimes \dots \otimes \left(\frac{\sigma_3}{2}\right)_i \otimes \dots \otimes 1$  where the sum is over the possible positions of the Pauli matrix.



Note that since  $r$  and  $s$  are non-negative and no larger than  $2j$ , the usual condition on  $m$ ,  $-j \leq m \leq j$ , is automatically satisfied.

Though a bit more involved, the same procedure goes through for the  $\hat{J}^2$  operator. It is built from the sum of products of operators  $\hat{J}^2 = \hat{J}_x^2 + \hat{J}_y^2 + \hat{J}_z^2$ . Acting once with the appropriate Pauli operators, one finds

$$\begin{aligned} \hat{J}^2 |jm\rangle \sim & \hbar \frac{\hat{\sigma}_1}{2} \left[ \frac{r}{2} \begin{array}{c} | \\ r+s \\ / \quad \backslash \\ r-1 \quad s+1 \\ \oplus \quad \ominus \end{array} + \frac{s}{2} \begin{array}{c} | \\ r+s \\ / \quad \backslash \\ r+1 \quad s-1 \\ \oplus \quad \ominus \end{array} \right] + \hbar \frac{\hat{\sigma}_2}{2} \left[ \frac{ir}{2} \begin{array}{c} | \\ r+s \\ / \quad \backslash \\ r-1 \quad s+1 \\ \oplus \quad \ominus \end{array} - \frac{is}{2} \begin{array}{c} | \\ r+s \\ / \quad \backslash \\ r+1 \quad s-1 \\ \oplus \quad \ominus \end{array} \right] \\ & + \hbar \frac{\hat{\sigma}_3}{2} \frac{(r+s)}{2} \begin{array}{c} | \\ r+s \\ / \quad \backslash \\ r \quad s \\ \oplus \quad \ominus \end{array}. \end{aligned}$$

Acting once again, some happy cancellation occurs and the result is

$$\hat{J}^2 |jm\rangle = \frac{\hbar^2}{2} \left( \frac{r^2 + s^2}{2} + rs + r + s \right) |jm\rangle$$

which equals the familiar  $j(j+1)$ . Actually, there is a pretty identity which gives another route to this result. The Pauli matrices satisfy [14]

$$\frac{1}{2} \sum_{i=1}^3 \sigma_{iA}^B \sigma_{iC}^D = \begin{array}{c} B \\ \diagdown \quad \diagup \\ A \quad C \end{array} \quad (11)$$

so the product is a 2-line. Similarly, the  $\hat{J}^2$  operator may be expressed as a 2-line. As will be shown in Section 5 this simplifies the above calculation considerably.

#### 4. A BIT OF GROUP THEORY

As we have seen, spin networks, inspired by expressing simple  $\delta$  and  $\epsilon$  matrices in terms of diagrams, are closely related to the familiar angular momentum representation of quantum mechanics. This section makes a brief excursion into group theory to exhibit two results which take a clear diagrammatic form, Schur's Lemma and the Wigner-Eckart Theorem.

Readers with experience with some group theory may have noticed that spin network edges are closely related to the irreducible representations of  $SU(2)$ . The key difference is that, on account of the sign conventions chosen in Section 2.1, the usual symmetrization of representations is replaced by the antisymmetrization of Eq. (6). In fact, each edge of the spin network is an irreducible representation. The tags on the edges can identify how these are generated – through the spatial dependence of a phase, for instance.

Since this diagrammatic algebra is designed to handle the combinations of irreducible representations, all the familiar results of representation theory have a diagrammatic form. For instance, Schur's Lemma states that any matrix  $T$  which commutes with two (inequivalent) irreducible representations  $D_g$  and  $D'_g$  of dimensions  $a+1$  and  $b+1$  is either zero or a multiple of the identity matrix

$$TD_g = D'_g T \text{ for all } g \in G \implies T = \begin{cases} 0 & \text{if } a \neq b \\ \lambda & \text{if } a = b \end{cases}.$$

Diagrammatically, this is represented as

$$\begin{array}{c} | \\ a \\ \circlearrowleft T \\ | \\ b \end{array} = \lambda \delta_a^b \left\{ \begin{array}{c} | \\ a \end{array} \right\}, \text{ where } \lambda = \frac{\begin{array}{c} | \\ a \\ \circlearrowleft \\ | \\ a \end{array}}{\Delta_a}.$$

The constant of proportionality is given by  $\lambda$  which, being a closed diagram, evaluates to a number.

The Wigner-Eckart theorem also takes a nice form in the diagrammatic language, providing an intuitive and fresh perspective on the theorem. It can help those who feel lost in the mire of irreducible tensor operators, reduced matrix elements, and Clebsch-Gordon coefficients. A general operator  $T_m^j$  grasping a line in the  $j_1$  representation ( $2j_1$  lines) to give a  $j_2$  representation is expressed as

$$m \text{---} \boxed{\text{T}} \text{---} 2j_1 \begin{array}{c} m_2 \\ | \\ 2j_2 \\ | \\ 2j_1 \\ | \\ m_1 \end{array} \sim \langle j_2 m_2 | T_m^j | j_1 m_1 \rangle.$$

Just from this diagram and the properties of the trivalent vertex, it is already clear that

$$|j_1 - j_2| \leq j \leq j_1 + j_2.$$

Likewise it is also the case that

$$m_2 = m_1 + m.$$

These results are the useful “selection rules” which are often given as a corollary to the Wigner-Eckart theorem. Notice that the operator expression is a diagram with the three legs  $j$ ,  $j_1$ , and  $j_2$ . This suggests that it might be possible to express the operator as a multiple of the basic trivalent vertex.<sup>9</sup> Defining

$$\begin{array}{c} 2j_2 \\ | \\ \text{T} \\ | \\ 2j_1 \end{array} \text{---} 2j_1 \quad := \quad \begin{array}{c} m \\ | \\ 2j_2 \\ | \\ 2j_1 \end{array} \text{---} m, \quad ,$$

one can combine the two lower legs together with Eq. (21). Applying Schur’s Lemma, one finds

$$\begin{array}{c} 2j_2 \\ | \\ \text{T} \\ | \\ 2j_1 \end{array} \text{---} 2j_1 = \sum_{c=|j-j_1|}^{j+j_1} \frac{\Delta_c}{\theta(2j, 2j_1, c)} \begin{array}{c} 2j_2 \\ | \\ \text{T} \\ | \\ 2j_1 \end{array} \text{---} 2j_1 = \omega \begin{array}{c} 2j_2 \\ | \\ \text{T} \\ | \\ 2j_1 \end{array}, \quad (12)$$

where

$$\omega = \frac{1}{\theta(2j, 2j_1, 2j_2)} \begin{array}{c} \text{T} \\ | \\ \text{T} \\ | \\ \text{T} \end{array}.$$

This relation expresses the operator in terms of a multiple of the trivalent vertex. It also gives a computable expression of the multiplicative factor. Comparing the first and last terms with the usual form of the theorem –<sup>10</sup>

$$\langle j_2 m_2 | T_m^j | j_1 m_1 \rangle = \langle j_2 | |T_m^j| | j_1 \rangle \langle j m j_1 m_1 | j_2 m_2 \rangle$$

– one can immediately see that the reduced matrix element  $\langle j_2 | |T_m^j| | j_1 \rangle$  is the  $\omega$  of Eq. (12). In this manner, any invariant tensor may be represented as a labeled, trivalent graph.

## 5. QUANTUM GEOMETRY: AREA OPERATOR

In this final example of the spin network diagrammatic algebra, the spectrum of the area operator of quantum gravity is derived. Before beginning, I ought to remark that the hard work of defining what is meant by the quantum area operator is not done here. The presentation instead concentrates on the calculation of the spectrum.

There are many approaches to constructing a quantum theory of gravity. The plethora of ideas arises in part from the lack of experimental guidance and in part from the completely new setting of general relativity for the techniques of quantization. One promising direction arises out of an effort to construct a background-independent theory which meets the requirements of quantum mechanics.

<sup>9</sup>Since the Clebsch-Gordan symbols are complete, any map from  $a \otimes b$  to  $c$  must be a multiple of the Clebsch-Gordan or  $3j$ -symbol.

<sup>10</sup>See, for instance, Reference [15] pg. 573 or Reference [16] pg. 116.

This field may be called “loop quantum gravity” or “spinet gravity.” (See Ref. [19] for a recent review.) The key idea in this approach is to lay aside the perturbative methods usually employed and, instead, directly quantize the Hamiltonian theory. Recently this field has bloomed. There is now a mathematically rigorous understanding of the kinematics of the theory and a number of (in principle testable) predictions of quantum geometry. One of the intriguing results of this study of quantum geometry is the discrete nature of space.

In general relativity the degrees of freedom are encoded in the metric on spacetime. However, it is quite useful to use new variables to quantize the theory [17]. Instead of a metric, in the canonical approach the variables are an “electric field,” which is the “square root” of the spatial metric, and a vector potential. The electric field  $\mathbf{E}$  is not only vector but also takes  $2 \times 2$  matrix values in an “internal” space. This electric field is closely related to the coordinate transformation from curved to flat coordinates (a triad). The canonically conjugate  $\mathbf{A}$ , usually taken to be the configuration variable, is similar to the electric vector potential but is more appropriately called a “matrix potential” for  $\mathbf{A}$  also is matrix valued. It determines the effects of geometry on spin- $\frac{1}{2}$  particles as they are moved through space.<sup>11</sup> (See Refs. [18] and [19] for more on the new variables.) States of loop quantum gravity are functions of the potential  $\mathbf{A}$ . A convenient basis is built from kets  $|s\rangle$  labeled by spin networks  $s$ . In this application of spin networks, they have special tags or weights on the edges of the graph. Every strand  $e$  of the gravitational spin network has the “phase” associated to it.<sup>12</sup> An orientation along every edge helps to determine these phases or weights. The states of quantum geometry are encoded in the knottedness and connectivity of the spin networks.

In classically gravity the area of a surface  $S$  is the integral

$$A_S = \int_S d^2x \sqrt{g},$$

in which  $g$  is the determinant of the metric on the surface.<sup>13</sup> The calculation simplifies if the surface is specified by  $z = 0$  in an adapted coordinate system. Expressed in terms of  $\mathbf{E}$ , the area of a surface  $S$  only depends on the  $z$ -vector component [6] - [9]

$$A_S = \int_S d^2x \sqrt{E_z \cdot E_z}. \quad (13)$$

The dot product is in the “internal” space. It is the same product between Pauli matrices as appears in Eq. (11). In the spin network basis  $\mathbf{E}$  is the momentum operator. As  $p \rightarrow -i\hbar \frac{d}{dx}$  in quantum mechanics, the electric field analogously becomes a “hand,”  $\mathbf{E} \rightarrow -i\hbar\kappa \overrightarrow{\square}_{-2 \rightarrow}$ . The  $\tau$  is proportional to a Pauli matrix,  $\tau = \frac{i}{2}\sigma$ . The  $\kappa$  factor is a sign: It is positive when the orientations on the edge and surface are the same, negative when the edge is oriented oppositely from the surface, and vanishes when the edges is tangent to the surface. The  $\mathbf{E}$  operator acts like the angular momentum operator  $\hat{J}$ . Since the  $\mathbf{E}$  operator vanishes unless it grasps an edge, the operator only acts where the spin network intersects the surface.

The square of the area operator is calculated first. Calling the square of the integrand of Eq. (13)  $\hat{O}$ , the two-handed operator at one intersection is

$$\hat{O} |s\rangle = - \sum_{e_I, e_J} \kappa_I \kappa_J \hat{J}_I \cdot \hat{J}_J |s\rangle \quad (14)$$

<sup>11</sup>For those readers familiar with general relativity the potential determines the parallel transport of spin- $\frac{1}{2}$  particles.

<sup>12</sup>In more detail, every edge has a “holonomy,” or path ordered exponential (i.e.  $\mathcal{P} \exp \int_e dt \dot{e}(t) \cdot \mathbf{A}(e(t))$ ) associated to it. See, for example, Ref. [18].

<sup>13</sup>The flavor of such an additional dependence is already familiar in flat space intergrals in spherical coordinates:

$$A = \int r^2 \sin(\theta) d\phi d\theta.$$



FIGURE 1. Two types of intersections of a spin network with a surface (a.) One isolated edge  $e$  intersects the surface transversely. The normal  $\hat{n}$  is also shown. (b.) One vertex of a spin network lies in the surface. All the non-tangent edges contribute to the area. Note that the network can be knotted.

where the sum is over edges  $e_I$  at the intersection. Here,  $\hat{J}_I$  denotes the vector operator  $\hat{J} = \hat{J}_x + \hat{J}_y + \hat{J}_z$  acting on the edge  $e_I$ . This  $\hat{O}$  is almost  $\hat{J}^2$  but for the sign factors  $\kappa_I$ . The area operator is the sum over contributions from all parts of the spin network which thread through the surface. In terms of  $\hat{O}$  over all intersections  $i$

$$\hat{A}_S |s\rangle = \frac{G}{4c^3} \sum_i \hat{O}_i^{1/2} |s\rangle,$$

including the dimensional constants.

As a first step, one can calculate the action of the operator  $\hat{O}$  on an edge  $e$  labeled by  $n$  as depicted in Figure 5(a.). In this case, the hands act on the same edge so the sign is 1,  $\kappa_I^2 = 1$ , and the angle operator squared becomes proportional to  $\hat{J}^2$ ! In the calculation one may make use of the Pauli matrix identity of Eq. (11)

$$\begin{aligned} \hat{O}_e |s\rangle &= -\hat{J}^2 |s\rangle \\ &= -\hbar^2 \frac{n^2}{2} \left( \text{bubble diagram} \right) |s - e\rangle. \end{aligned}$$

The edge is shown in the the diagram so it is removed spin network  $s$  giving the state  $|s - e\rangle$ . Now the diagram may be reduced using the recoupling identities. The bubble may be extracted with Eq. (18)

$$\begin{aligned} \hat{O}_e |s\rangle &= -\hbar^2 \frac{n^2}{2} \left( \text{bubble diagram} \right) |s - e\rangle \\ &= -\hbar^2 \frac{n^2}{2} \frac{\theta(n, n, 2)}{\Delta_n} \left( \text{bubble diagram} \right) |s - e\rangle \\ &= -\hbar^2 \frac{n^2}{2} \left( -\frac{n+2}{2n} \right) |s\rangle \\ &= \hbar^2 \frac{n(n+2)}{4} |s\rangle, \end{aligned}$$

in which Eq. (17) was also used in the second line. Putting this result into the area operator, one learns that the area coming from all the transverse edges is [6]

$$\begin{aligned} \hat{A}_S |s\rangle &= \frac{G\hbar}{c^3} \sum_i \sqrt{\frac{n_i(n_i+2)}{4}} |s\rangle \\ &= l_P^2 \sum_i \sqrt{j_i(j_i+1)} |s\rangle. \end{aligned} \tag{15}$$

The units  $\hbar$ ,  $c$ , and  $G$  are collected into the Planck length  $l_P = \sqrt{\frac{G\hbar}{c^3}} \sim 10^{-35} m$ . The result is also re-expressed in terms of the more familiar angular momentum variables  $j = \frac{n}{2}$ .

The full spectrum of the area operator is found by considering all the intersections of the spin network with the surface  $S$  including vertices which lie on the surface as in Figure 5(b.). Summing over all contributions [8]

$$\hat{A}_S | s \rangle = \frac{l_P^2}{2} \sum_v [2j_v^u(j_v^u + 1) + 2j_v^d(j_v^d + 1) - j_v^t(j_v^t + 1)]^{1/2} | s \rangle$$

in which  $j_v^\kappa$  ( $j_v^d$ ) is the total spin with a positive (negative) sign  $\kappa$  and  $j_v^t$  is the total spin of edges tangent to the surface at the vertex  $v$ .

This result is utterly remarkable in that the calculation predicts that space is discrete. Measurements of area can only take these quantized values. As is the case in many quantum systems there is a “jump” from the lowest possible non-zero value. This “area quanta” is  $\frac{\sqrt{3}}{4}l_P^2$ . In an analogous fashion, as for an electron in a hydrogen atom, surfaces make a quantum jump between states in the spectrum of the area operator.

## 6. SUMMARY

This introduction to spin networks diagrammatics offers a view of the diversity of this structure. Touching on knot theory, group theory, and quantum gravity this review gives a glimpse of the applications. These techniques also offer a new perspective on familiar angular momentum representations of undergraduate quantum mechanics. As shown with the area operator in the last section, it is these same techniques which are a focus of frontier research in the Hamiltonian quantization of the gravitational field.

**Acknowledgment.** *It is a pleasure to thank Franz Hinterleitner and Johnathan Thornburg for comments on a draft of the primer. I gratefully acknowledge support of the FWF through a Lise Meitner Fellowship.*

## APPENDIX A. LOOPS, THETAS, TETS AND ALL THAT

This appendix contains the basic definitions and formulae of diagrammatic recoupling theory using the conventions of Kauffman and Lins [12] – a book written in the context of the more general Temperley-Lieb algebra .

The function  $\theta(m, n, l)$  is given by

$$\theta(m, n, l) = \left( \begin{matrix} m \\ -n \\ l \end{matrix} \right) = (-1)^{(a+b+c)} \frac{(a+b+c+1)!a!b!c!}{(a+b)!(b+c)!(a+c)!} \quad (16)$$

where  $a = (l + m - n)/2$ ,  $b = (m + n - l)/2$ , and  $c = (n + l - m)/2$ . An evaluation which is useful in calculating the spectrum of the area operator is  $\theta(n, n, 2)$ , for which  $a = 1$ ,  $b = n - 1$ , and  $c = 1$ .

$$\theta(n, n, 2) = (-1)^{(n+1)} \frac{(n+2)!(n-1)!}{(2n!)^2} = (-1)^{(n+1)} \frac{(n+2)(n+1)}{2n}. \quad (17)$$

A “bubble” diagram is proportional to a single edge.

$$\begin{matrix} h \\ \circlearrowleft \\ a \quad b \\ l \end{matrix} = \delta_{nl} \frac{(-1)^n \theta(a, b, n)}{(n+1)} \begin{matrix} | \\ n \\ | \end{matrix}. \quad (18)$$

The basic recoupling identity relates the different ways in which three angular momenta, say  $a$ ,  $b$ , and  $c$ , can couple to form a fourth one,  $d$ . The two possible recouplings are related by

$$\begin{matrix} \circlearrowleft \\ b \quad c \\ a \quad d \end{matrix} = \sum_{|a-b| \leq i \leq (a+b)} \left\{ \begin{matrix} a & b & i \\ c & d & i' \end{matrix} \right\} \begin{matrix} \circlearrowleft \\ b \quad c \\ a \quad d \end{matrix} \quad (19)$$

where on the right hand side is the  $6j$ -symbol defined below. It is closely related to the  $Tet$  symbol. This is defined by [12]

$$\begin{aligned}
 \begin{array}{c} \triangle \\ \text{---} \\ \triangle \end{array} &= \begin{array}{c} \text{---} \\ \text{---} \\ \text{---} \end{array} = Tet \begin{bmatrix} a & b & e \\ c & d & f \end{bmatrix} \\
 Tet \begin{bmatrix} a & b & e \\ c & d & f \end{bmatrix} &= N \sum_{m \leq s \leq S} (-1)^s \frac{(s+1)!}{\prod_i (s-a_i)! \prod_j (b_j-s)!} \\
 N &= \frac{\prod_{i,j} [b_j - a_i]!}{a!b!c!d!e!f!}
 \end{aligned} \tag{20}$$

in which

$$\begin{aligned}
 a_1 &= \frac{1}{2}(a+d+e) & b_1 &= \frac{1}{2}(b+d+e+f) \\
 a_2 &= \frac{1}{2}(b+c+e) & b_2 &= \frac{1}{2}(a+c+e+f) \\
 a_3 &= \frac{1}{2}(a+b+f) & b_3 &= \frac{1}{2}(a+b+c+d) \\
 a_4 &= \frac{1}{2}(c+d+f) & m &= \max \{a_i\} \quad M = \min \{b_j\}
 \end{aligned}$$

The  $6j$ -symbol is then defined as

$$\left\{ \begin{array}{ccc} a & b & i \\ c & d & j \end{array} \right\} := \frac{Tet \begin{bmatrix} a & b & i \\ c & d & j \end{bmatrix} \Delta_i}{\theta(a,d,i) \theta(b,c,i)}.$$

These satisfy a number of properties including the orthogonal identity

$$\sum_l \left\{ \begin{array}{ccc} a & b & l \\ c & d & j \end{array} \right\} \left\{ \begin{array}{ccc} d & a & i \\ b & c & l \end{array} \right\} = \delta_i^j$$

and the Biedenharn-Elliot or Pentagon identity

$$\sum_l \left\{ \begin{array}{ccc} d & i & l \\ e & m & c \end{array} \right\} \left\{ \begin{array}{ccc} a & b & f \\ e & l & i \end{array} \right\} \left\{ \begin{array}{ccc} a & f & k \\ d & d & l \end{array} \right\} = \left\{ \begin{array}{ccc} a & b & k \\ c & d & i \end{array} \right\} \left\{ \begin{array}{ccc} k & b & f \\ e & m & c \end{array} \right\}.$$

Two lines may be joined via

$$\begin{array}{c} \text{---} \\ \text{---} \\ \text{---} \end{array} = \sum_c \frac{\Delta_c}{\theta(a,b,c)} \begin{array}{c} \text{---} \\ \text{---} \\ \text{---} \end{array}. \tag{21}$$

One also has occasion to use the coefficient of the “ $\lambda$ -move”

$$\begin{array}{c} \text{---} \\ \text{---} \\ \text{---} \end{array} = \lambda_c^{ab} \begin{array}{c} \text{---} \\ \text{---} \\ \text{---} \end{array} \quad \text{where } \lambda_c^{ab} \text{ is} \\
 \lambda_c^{ab} = (-1)^{(a+b-c)/2}. \tag{22}$$

## REFERENCES

- [1] Roger Penrose, “Angular momentum: An approach to combinatorial spacetime” in *Quantum Theory and Beyond* T. Bastin, ed. (Cambridge University Press, Cambridge, 1971); “Combinatorial Quantum Theory and Quantized Directions” in *Advances in Twistor Theory*, Research Notes in Mathematics 37, L. P. Hughston and R. S. Ward, eds. (Pitman, San Francisco, 1979) pp. 301-307; “Theory of Quantized Directions,” unpublished notes.
- [2] Carlo Rovelli and Lee Smolin, “Spin Networks and Quantum Gravity,” *Phys. Rev. D* **52** 5743-5759 (1995).
- [3] John C. Baez, “Spin networks in gauge theory,” *Advances in Mathematics* **117** 253 - 272 (1996), Online Preprint Archive: <http://xxx.lanl.gov/abs/gr-qc/9411007>; “Spin Networks in Nonperturbative Quantum Gravity,” in *The Interface of Knots and Physics*, Louis Kauffman, ed. (American Mathematical Society, Providence, Rhode Island, 1996), pp. 167 - 203, Online Preprint Archive: <http://xxx.lanl.gov/abs/gr-qc/9504036>.
- [4] Ernst Mach, *Fichtes Zeitschrift für Philosophie* **49** 227 (1866). Cited in Lee Smolin in *Conceptual Problems of Quantum Gravity*, A. Ashtekar and J. Stachel, eds. (Birkhäuser, Boston, 1991).

- [5] John P. Moussouris, “Quantum models as spacetime based on recoupling theory,” Oxford Ph.D. dissertation, unpublished (1983).
- [6] Carlo Rovelli and Lee Smolin, “Discreteness of area and volume in quantum gravity,” *Nuc. Phys. B* **442**, 593-622 (1995).
- [7] Roberto De Pietri and Carlo Rovelli, “Geometry eigenvalues and the scalar product from recoupling theory in loop quantum gravity,” *Phys. Rev. D* **54**(4), 2664-2690 (1996).
- [8] Abhay Ashtekar and Jerzy Lewandowski, “Quantum Theory of Geometry I: Area operators,” *Class. Quant. Grav.* **14**, A55-A81 (1997).
- [9] S. Frittelli, L. Lehner, C. Rovelli, “The complete spectrum of the area from recoupling theory in loop quantum gravity,” *Class. Quant. Grav.* **13**, 2921-2932 (1996).
- [10] K. Reidemeister, *Knotentheorie* (Chelsea Publishing Co., New York, 1948), original printing (Springer, Berlin, 1932). See also Louis Kauffman, *Knots and Physics*, pp. 16.
- [11] Louis H. Kauffman, *Knots and Physics*, Series on Knots and Everything - Vol. 1 (World Scientific, Singapore, 1991) pp. 125-130, 443-471.
- [12] Louis H. Kauffman and Sóstenes L. Lins, *Temperley-Lieb Recoupling Theory and Invariants of 3-Manifolds*, Annals of Mathematics Studies N. 134, (Princeton University Press, Princeton, 1994), pp. 1-100.
- [13] Carlo Rovelli and Lee Smolin, “Loop Representation of quantum general relativity,” *Nuc. Phys. B* **331**(1), 80-152 (1990).
- [14] R. DePietri, “On the relation between the connection and the loop representation of quantum gravity,” *Class. Quant. Grav.* **14** 53-70 (1990).
- [15] Albert Messiah, *Quantum Mechanics*, Vol. 2 (John Wiley, New York, 1966).
- [16] H.F. Jones, *Groups, Representations and Physics* (Adam Hilger, Bristol, 1990).
- [17] Abhay Ashtekar, “New variables for classical and quantum gravity,” *Phys. Rev. Lett.* **57**(18), 2244-2247 (1986); *New perspectives in canonical gravity* (Bibliopolis, Naples, 1988); *Lectures on non-perturbative canonical gravity*, Advanced Series in Astrophysics and Cosmology-Vol. 6 (World Scientific, Singapore, 1991).
- [18] Abhay Ashtekar, “Quantum mechanics of Riemannian geometry,” [http://vishnu.nirvana.phys.psu.edu/riem\\_qm/riem\\_qm.html](http://vishnu.nirvana.phys.psu.edu/riem_qm/riem_qm.html).
- [19] Carlo Rovelli, “Loop Quantum Gravity,” *Living Reviews in Relativity* <http://www.livingreviews.org/Articles/Volume1/1998-1rovelli>; “Strings, Loops, and Others: A critical survey of the present approaches to quantum gravity,” in *Gravitation and Relativity: At the turn of the Millennium*, Proceedings of the GR-15 Conference, Naresh Dadhich and Jayant Narlikar, ed. (Inter-University Center for Astronomy and Astrophysics, Pune, India, 1998), pp. 281 - 331, Online Preprint Archive: <http://xxx.lanl.gov/abs/gr-qc/9803024>.